Journal of Hazardous Materials 175 (2010) 138–145

Contents lists available at ScienceDirect

Journal of Hazardous Materials

journal homepage: www.elsevier.com/locate/jhazmat

Mechanism and kinetics of parathion degradation under ultrasonic irradiation

Juan-Juan Yao*, Nai-Yun Gao, Cong Li, Lei Li, Bin Xu

State Key laboratory of Pollution Control and Resources Reuse, Tongji University, Shanghai, 200092, China

ARTICLE INFO

Article history:
Received 5 May 2009
Received in revised form
27 September 2009
Accepted 28 September 2009
Available online 2 October 2009

Keywords:
Parathion degradation
Ultrasonic irradiation
Kinetic model
Heterogeneous reaction
Pathways
Molecular orbital theory

ABSTRACT

The parathion degradation under ultrasonic irradiation in aqueous solution was investigated. The results indicate that at the conditions in question, degradation rate of parathion decreased with increasing initial concentration and decreasing power. The optimal frequency for parathion degradation was 600 kHz. The free radical reactions predominate in the sonochemical degradation of parathion and the reaction zones are predominately at the bubble interface and, to a much lesser extent, in bulk solution. The gas/liquid interfacial regions are the real effective reaction sites for sonochemical degradation of parathion. The reaction can be well described as a gas/liquid heterogeneous reaction which obeys a kinetic model based on Langmuir–Hinshelwood model. The main pathways of parathion degradation by ultrasonic irradiation were also proposed by qualitative and quantitative analysis of organic and inorganic byproducts. It is indicated that the N_2 in air takes part in the parathion degradation through the formation of $^{\bullet}NO_2$ under ultrasonic irradiation. Parathion is decomposed into paraoxon and 4-nitrophenol in the first step via two different pathways, respectively, which is in agreement with the theoretical molecular orbital (MO) calculations.

1. Introduction

Organophosphorus pesticides (OPs) are widely applied for plant and crop protection and frequently detected in surface water and groundwater with concentrations at ng/L to μg/L levels [1,2]. The toxicity of OPs is due to the non-specific inhibition of enzyme acetylcholinesterase (AChE) in the nervous system. Most OPs containing P=S double bonds. When parathion is applied in agricultural activities or transports into surface water, it is readily oxidized to paraoxon (P=O), a more potent AChE inhibitor [3,4]. Moreover, the oxidation is even more efficient during disinfection of potable water when chlorine is used [5,6]. For this reason, there is a great interest in research for OPs degradation and their pathways.

Recently, ultrasonic irradiation as a potential advanced oxidation process has received increasing attentions for the degradation of various organic pollutants commonly found in water, such as pesticide [7,8], dye [9,10], endocrine disrupter compounds [11,12], POPs [13,14], perfluorinated chemicals [15,16], odor-causing compound [17], pharmaceuticals [18,19] and microcystins [20]. Sonolytic degradation of pollutants occurs as a result of continuous formation and collapse of cavitation bubbles on a microsecond time scale. Accompanied with the bubble collapse, hot nucleus is formed, characterized with extremely high temperatures (thousands of degrees) and pressure (hundreds of atmospheres). In aqueous solution under ultrasonic irradiation, three different reaction zones have been postulated [21–23]: (i) interiors of collapsing cavities where water vapor is pyrolyzed to hydroxyl radicals ($^{\bullet}OH$) and hydrogen atoms ($^{\bullet}H$), as shown in Eq. (1), and where gas-phase pyrolysis and/or combustion reactions of volatile substances dissolved in water occur.

$$H_2O \xrightarrow{\text{Ultrasonic Irradiation}} H^{\bullet} + {}^{\bullet}OH \quad (1)$$

(ii) Interfacial regions between cavitational bubbles and the bulk solution. Though the temperature here is lower than one within the bubbles, an adequately high temperature with a high gradient exists in these regions, and locally condensed $^{\bullet}OH$ has been reported to be formed here [24]. (iii) Bulk solution at ambient temperature where reactions with $^{\bullet}OH$ or $^{\bullet}H$ that migrates from the interface occur.

However, as a kind of typical organophosphorus pesticides, there are little literatures about the mechanism and kinetics of parathion degradation under ultrasonic irradiation. Sonolysis of parathion was reported first by Kotronarou et al. [25] who identified the final products and proposed a simple degradation pathway. Wang et al. [26–28] focused on the research about sonocatalytic degradation of parathion and methyl parathion under low frequency ultrasonic irradiation in the presence of nanometer materials, but did not propose the detailed degradation pathways and kinetics.

In this study, sonochemical degradation of parathion is investigated. The objectives of this study are to: (i) evaluate the effect of operational parameters on parathion degradation; (ii) propose

* Corresponding author. Tel.: +86 21 65982691; fax: +86 21 65986313.
E-mail address: yao_juanjuan@yahoo.cn (J.-J. Yao).

0304-3894/$ – see front matter © 2009 Elsevier B.V. All rights reserved.
doi:10.1016/j.jhazmat.2009.09.140

the degradation pathways and kinetics and (iii) explain the initial pathways by the molecular orbital theory.

2. Experimental

2.1. Chemicals

Parathion (99%, purity), paraoxon (99%, purity) and triethyl phosphate (99%, purity) were from Dr. Ehrenstorfer (German). Acetonitrile (HPLC), benzoquinone (99%), dichloromethane (PESTANAL), 2,4-dinitrophenol standard solution, methanol (HPLC), 4-nitrophenol standard solution and triphenylphosphate (>99%) as internal standard (I.S.) obtained from Sigma–Aldrich (USA). All the other reagents are analytical grade and used without further treatment. All solutions used were prepared daily with water purified by Milli-Q Gradient water purification system.

2.2. Experiments

Sonochemical reactions were conducted with a series of ultrasonic generators which operated with a fixed frequency of 200, 400, 600 and 800 kHz, respectively. Electric power outputs are up to 100 W (Institute of Acoustics, Chinese Academy of Sciences). The reactions were carried out in an open cylindrical stainless steel reaction vessel (diameter: 100 mm, height: 200 mm), which is directly connected to the ultrasonic transducer (diameter: 80 mm) with flanges and a flexible Teflon O-ring for seal. The vessel is immersed in a water bath, which is connected to a temperature control unit. All tests were performed at $25.0 \pm 1.0\,^{\circ}C$ and under atmospheric pressure. In all experiments, 300.0 mL of parathion solution were prepared on the spot and then put into the reaction vessel. The pH value of the original parathion solution was adjusted to 7.00 (±0.05) with 1.0 M HCl and 1.0 M NaOH, and remained uncontrolled during the ultrasonic irradiation, except in the experiments to investigate the effect of HCO_3^- in which the initial pH was not adjusted. Each experiment repeated three times. The standard deviations of triplicate experiments were less than 5%.

2.3. Analysis

In order to identify parathion degradation byproducts, the solid-phase extraction (SPE) method was applied for the samples extraction. 50.0 mL samples after sonochemical treatment were extracted by using Supelclean LC-18 cartridge (500 mg/3 mL). Prior to the extraction, the samples were acidified to pH 2.0 with 1 M HCl. The cartridges were conditioned by 5.0 mL acetonitrile, 5.0 mL methanol and then 10.0 mL water (pH 2). After the passage of the samples, the cartridges were vacuum dried for 30.0 min. The cartridges were then washed twice with 5.0 mL methanol. The extracts were evaporated to dryness and re-dissolved in 1.0 mL dichloromethane before being analyzed by gas chromatography/electron impact mass spectrometry (GC/EI-MS). A Shimadzu GC/MS-QP2010 gas chromatograph–mass spectrometer equipped with a 30 m RTX-5MX column (thickness: 0.25 μm, diameter: 0.25 mm) was used to identify degradation byproducts. Helium (>99.999%) was used as the carrier gas, with a flow rate of 1.5 mL/min. The GC oven temperature program was: initial temperature at 35.0 °C for 1 min, 8.0 °C min^{-1} gradient until 190.0 °C, 2.0 °C min^{-1} until 220.0 °C, 20 min^{-1} until 280.0 °C for 5 min. The identification of the byproducts was confirmed by comparing retention time as well as mass spectra of available standard samples and the interpretation of mass spectra of unknowns through NIST 02 mass spectral library searches.

In the parathion and paraoxon quantification experiments, samples after sonochemical treatment were extracted by dichloromethane. Internal standards were added in samples prior to extraction. A Shimadzu GC/MS-QP2010 mentioned above was used in simultaneous quantification of parathion and paraoxon with SIM mode. The GC oven temperature program was: initial temperature at 35 °C, hold for 1 min, 25.0 °C min^{-1} gradient until 200.0 °C, 10.0 °C min^{-1} until 220.0 °C, 30 min^{-1} until 270.0 °C, and hold for 3 min.

The ionic byproducts were analyzed using an ICS1000 ion chromatograph (Dionex Corporations, USA), equipped with an IonPacAS11 anion column and suppressed EDC detector using 20 mmol/L potassium hydroxide eluent.

4-Nitrophenol and 2,4-dinitrophenol were analyzed by a Shimadzu LC-2010AHT HPLC equipped with a VP-ODS column (250 mm × 4.6 mm) and ultraviolet detector setting wavelength of 318 nm. Elution was performed with a mobile phase composed of acetonitrile/water/acetic acid (50:49.6:0.4, v/v/v).

In order to verify the actual ultrasonic power, the energy dissipated by the transducer of ultrasonic device into solutions was calibrated by standard calorimetric procedures [29,30].

3. Results and discussions

3.1. Effect of ultrasonic frequency, power and initial concentration on parathion degradation

Ultrasonic frequency, power and initial concentration are three important parameters for sonochemical degradation of parathion.

Table 1
Pseudo-first-order rate constants for the sonochemical degradation of parathion under different operational condition and radical scavenger additions.

Frequency (kHz)	Initial concentration (μM)	Ultrasonic power (W)	TBA (M)	HCO_3^- (M)	k_{app} (min^{-1})	R^2
200	2.9	45	–	–	0.0771	0.996
400	2.9	45	–	–	0.133	0.998
600	2.9	45	–	–	0.150	0.996
800	2.9	45	–	–	0.0968	0.995
600	0.8	55.2	–	–	0.254	0.995
600	0.8	37.8	–	–	0.154	0.990
600	0.8	17.4	–	–	0.0660	0.996
600	2.9	55.2	–	–	0.192	0.998
600	2.9	37.8	–	–	0.102	0.996
600	2.9	17.4	–	–	0.0537	0.989
600	5.2	55.2	–	–	0.169	0.997
600	5.2	37.8	–	–	0.0808	0.993
600	5.2	17.4	–	–	0.0438	0.994
600	2.9	55.2	0.001	–	0.142	0.989
600	2.9	55.2	0.01	–	0.0195	0.985
600	2.9	55.2	0.1	–	0.0124	0.991
600	2.9	55.2	–	0.001	0.172	0.999
600	2.9	55.2	–	0.01	0.166	0.999
600	2.9	55.2	–	0.1	0.140	0.996

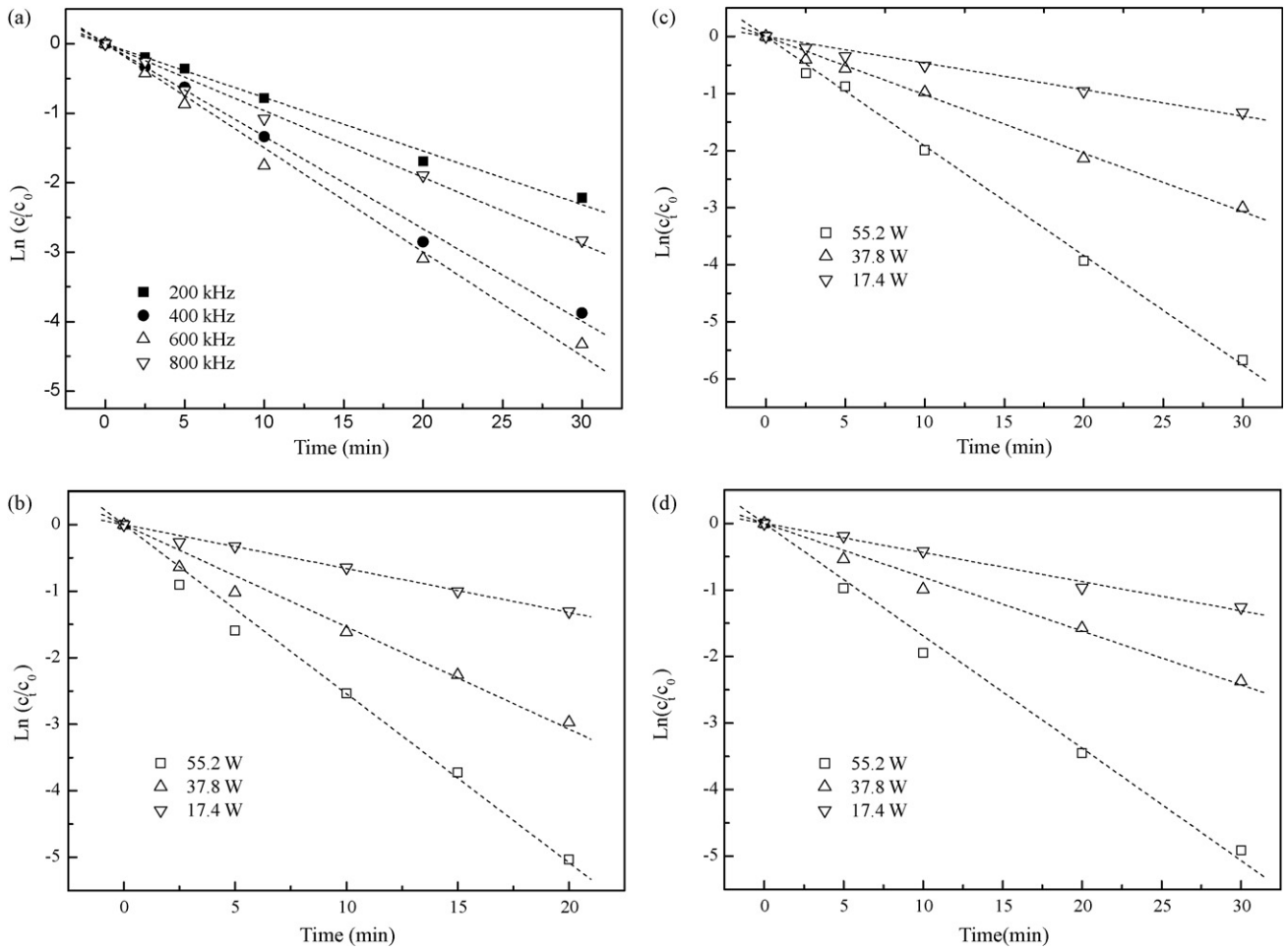

Fig. 1. Effect of ultrasonic frequency, power and initial concentration on parathion degradation. ((a) Parathion: 2.9 μM, ultrasonic power: 45.0 W; (b) parathion: 0.8 μM, ultrasonic frequency: 600 kHz; (c) parathion: 2.9 μM, ultrasonic frequency: 600 kHz; (d) parathion: 5.2 μM, ultrasonic frequency: 600 kHz.)

In order to evaluate the effect of operational parameters on parathion degradation, the pseudo-first-order kinetic model was used.

$$\ln \frac{c_t}{c_0} = -k_{app} t \quad (2)$$

where k_{app} is an apparent rate constant, and c_0 and c_t is parathion concentration at time 0 and t.

Based on Eq. (2), plots of $\ln(c_t/c_0)$ versus irradiation time (t) were prepared as shown in Fig. 1(a)–(d) according to data obtained with different operating conditions. The pseudo-first-order rate constants, k_{app}, of parathion under different conditions are summarized in Table 1. In the experiments to discuss the effect of ultrasonic frequency on parathion degradation, the same ultrasonic power determined by standard calorimetric process, 45 W, was applied at each run to ensure comparative ultrasonic conditions at the different frequencies. k_{app} increased from 0.0771 to 0.150 min^{-1} with the increasing ultrasonic frequency from 200 to 600 kHz. However, k_{app} decreased to 0.0968 when the frequency went up to 800 kHz. The optimal frequency for parathion degradation was 600 kHz. In general, when the ultrasonic frequency increases, the resonant radius of the cavitation bubbles decreases to cause less violent bubble collapse and thus decreases the amounts of hydroxyl radicals in each collapse. However, the decreasing sizes of bubbles with the increasing frequency shorten the collapse duration, so that more collapses occur in a unit time and thus augment the overall amount of radicals [21]. Nevertheless, at very high frequencies, the cavitational effect is reduced because either the rarefaction cycle of the sound wave produces a negative pressure which is insufficient in its duration and/or intensity to initiate cavitation or the compression cycle occurs faster than the time for the microbubble to collapse [31]. Therefore, the optimal frequency can be found to produce the highest net concentration of free radicals. Previous research found that the •OH radical yield at different frequencies followed the order 354 > 620 > 803 > 206 > 1062 kHz [32]. Moreover, the higher frequency leads to a more efficient mass transfer owing to the faster flux of active radical species and bulk reactive solute toward the cavitation bubble interface [31]. Pétrier and Francony [33] compared the reaction rates of phenol (a nonvolatile and hydrophilic solute), and carbon tetrachloride (volatile and hydrophobic solute) in aqueous solutions at 20, 200, 500, and 800 kHz. The results showed that phenol degradation reached a maximum at 200 kHz, while the degradation rate of carbon tetrachloride increased with increasing frequency. However, Lesko et al. [34] found that the degradation of phenol was faster at 358 kHz than at 205, 618, or 1071 kHz and attributed this to the optimal •OH radical yield at 358 kHz. Hung and Hoffmann [35] investigated the degradation of carbon tetrachloride over a similar frequency range and observed the highest degradation rate at 618 kHz and attributed this to a more efficient mass transfer of reactive solute from the liquid phase to the vapor phase. Recently, Yang et al. [32] found that the optimal frequency for another nonvolatile solute, octylbenzene sulfonic acid (OBS), was 620 kHz at the frequency range of 206–1062 kHz and attributed this to the changes in the amount of OBS that can accumulate at the gas/liquid surface of cavitation bubbles in unit time. These results indicate that frequency effects are

dependent on the nature of the molecules and the reaction localization. As a nonvolatile and hydrophobic compound, parathion tends to migrate towards the bubble interface due to its lower water solubility (11 mg/L) [36] and higher octanol–water partition coefficient ($\log K_{ow}$ = 3.83) [36]. Therefore, the optimal frequency for parathion degradation is not only determined by the optimal •OH radicals yield but also the efficient mass transfer of molecule from the liquid phase to the gas/liquid interface.

k_{app} increased with the ultrasonic power increasing in the studied power range and initial concentration range. The beneficial effect of power on degradation rates is due to increased cavitational activity at higher levels of power. With power and the number of collapsing cavities increasing, degradation rates increase. It is noticed that k_{app} decreased with increasing initial solute concentration, which indicates that k_{app} is still a function of parathion concentration. Therefore, sonochemical degradation of parathion does not obey a real first-order kinetic model, just a pseudo one. Moreover, these same results are also obtained in the sonolytic degradation of pesticide [37], dyes [38], humic substances [39], chlorophenol [40], phenol [41] and surfactants [42].

3.2. Effect of hydroxyl radical scavengers on parathion degradation

Radical scavenger additions are often used to confirm the existent of a free radical mechanism. It can be concluded that a free radical reaction is involved if the degradation rates of chemicals considerably decrease in the presence of these scavengers. Tert-butyl alcohol (TBA) was applied as a free radicals scavenger for the gaseous regions and/or interfacial regions of the cavitation bubbles [20], and sodium bicarbonate was also chosen as a free radicals scavenger for bulk solution [43]. As the concentration of hydroxyl radical accumulated at a bubble interface to be 4×10^{-3} M [24], the scavengers were added in all the experiments with mM level.

Based on Eq. (2), plots of $\ln(c_t/c_0)$ versus irradiation time (t) were prepared as shown in Fig. 2(a) and (b). The pseudo-first-order rate constants of parathion degradation with different radical scavenger additions are summarized in Table 1. It is clearly indicated that k_{app} decreased and then reached stable situation with the concentration of TBA increasing. k_{app} with 0.01 M TBA addition was only one tenth of that without TBA. However, k_{app} decreased a little in the presence of bicarbonate ions with the concentration from 0.001 to 0.1 M. It is indicated that free radical reactions predominate in the parathion degradation under ultrasonic irradiation and the reaction zones are predominately at the interfacial regions between cavitation bubbles and bulk solution and, to a much lesser extent, in bulk solution. Meanwhile, hydrolysis commonly for ester at the interfacial regions is also involved. Previous researches [44–46] indicated ultrasonic can enhanced the hydrolysis of ester because a layer of hot water shell exists at the cavitation bubble interface and contributes to the accelerated hydrolysis.

3.3. Kinetics of parathion degradation under ultrasonic irradiation

According to the conclusions drawn from the above studies, the gas/liquid interfacial regions are the real effective reaction sites for sonochemical degradation of parathion. Therefore, the reaction can be described as a gas/liquid heterogeneous reaction. Langmuir–Hinshelwood (L–H) model which often applied to a kinetic analysis of heterogeneous gas/solid catalytic reactions can be introduced to simulate the reaction kinetics [37–40,42,47]. However, the model in the present studies has a different explanation

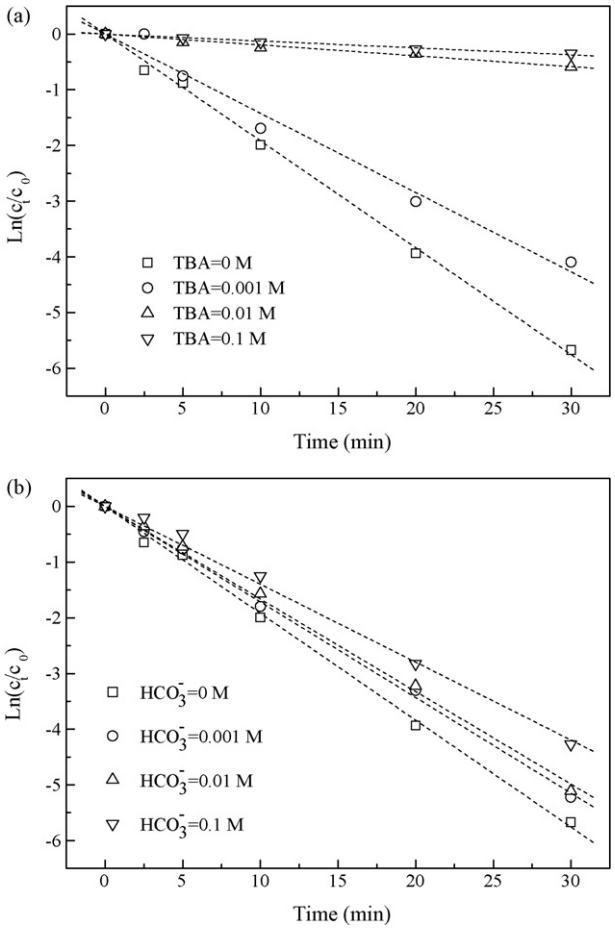

Fig. 2. Effect of hydroxyl radical scavengers on parathion degradation under ultrasonic irradiation. (Parathion: 2.9 μM; ultrasonic power: 55.2 W; frequency: 600 kHz. (a) TBA ; (b) HCO_3^-.)

from L–H model [38].

$$-\frac{dc}{dt} = r = \frac{kK_c}{1 + K_c} \tag{3}$$

where k (M^{-1} s) is an observed rate constant, c (M^{-1}) is parathion concentration and K (M^{-1}) is the equilibrium absorption constant of parathion toward the effective reaction site before the moment of bubble collapse.

Bases on the Eq. (3), plots of 1/initial r versus 1/initial parathion concentration are drawn as shown in Fig. 3.The data were well fitted by L–H based model, which further confirmed that the degradation of parathion occurs at the interfacial regions. The k value obtained at 600 kHz (2.141×10^{-8} M^{-1} s) is 2.00 times higher than that at 200 kHz (1.071×10^{-8} M^{-1} s). It is attributed to the much higher •OH yield at 600 kHz than 200 kHz [32]. However, the K value obtained at 200 kHz (160,239 M^{-1}) is 1.39 times higher than that at 600 kHz (115,630 M^{-1}). It is attributed to the delayed growth and long collapse duration of cavitation bubbles resulting in more solute accumulation at the bubble interface in a cavitational cycle.

When the chemical concentration c is a macromolar solution, namely, $K_c \ll 1$, the equation can be simplified to a pseudo-first-order equation:

$$-\frac{dc}{dt} = r = kKc = k_{app}c \tag{4}$$

Therefore, sonochemical degradation of parathion does not obey simple first-order kinetic model, but pseudo-first-order-kinetic model based on the heterogeneous reaction kinetic model.

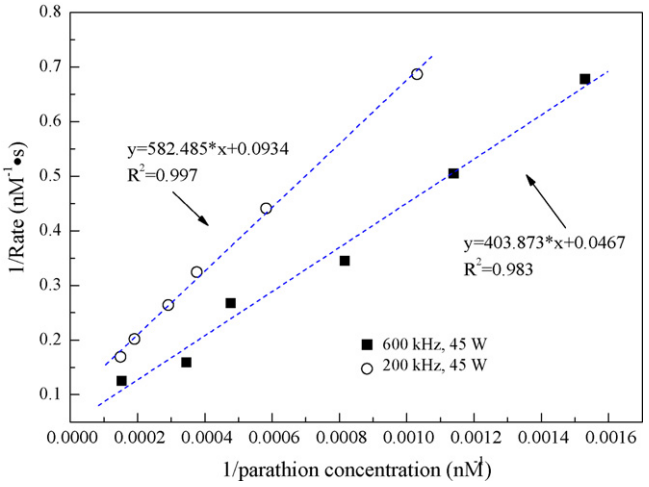

Fig. 3. Relationship between initial degradation rate of the parathion and initial concentration (ultrasonic power: 45.0 W; frequency: 600 kHz).

3.4. Byproducts analysis of sonochemical degradation of parathion

Up to 10 transformation products have been identified using GC–MS-EI detection (shown in Table 2). 4-Nitrophenol and 2,4-dinitrophenol were quantified by HPLC, while paraoxon by GC–MS (shown in Fig. 4(a)). At the beginning of degradation reaction, paraoxon was one of the major byproducts with the highest concentration accounting for 10% of decayed parathion via the replace of sulfur by oxygen in the P=S bond. Paraoxon is more potent AChE inhibitors than its parent compounds. Therefore, formation and degradation of paraoxon is an essential point in evaluating the effectiveness of toxicity reduction during the degradation of parathion. In the same reaction, 4-nitrophenol was the most abundant organic byproduct with the highest concentration accounting for 20% of the parent parathion. 2,4-Dinitrophenol was another important byproduct with the highest concentration accounting for 3.9% of the parent parathion. It is noticed that 2,4-dinitrophenol has never been detected in both photocatalysis and photolysis of parathion or methyl parathion [48–50].

The concentration of SO_4^{2-}, PO_4^{3-}, NO_3^- and NO_2^- were monitored during the sonochemical degradation process. As shown in Fig. 4(b), the concentration of SO_4^{2-} increased rapidly in the first 45 min and then stabilized, which corresponds to the degradation curve of parathion (shown in Fig. 4(a)). On the other hand, about 76% of the total sulfur initially present in the parathion was converted to SO_4^{2-} after 120 min. It was confirmed that the oxidation of parathion to paraoxon with formation of SO_4^{2-} is one of the first steps in the reaction pathway. Similar phenomena has also been reported in the TiO_2 photocatalysis of parathion due to the attack of the •OH on the P=S bond [51]. The formation of PO_4^{3-} was also observed after 5 min.The concentration of PO_4^{3-} increased steadily and finally about 27% of the total phosphorus initially present in the parathion was converted to PO_4^{3-} in the end. At the same reaction, an amount of NO_3^- and NO_2^- were also detected. The concentration of NO_2^- increased initially and up to a peak value of 162 μmol μL^{-1} around 45 min but then decreased, while the concentration of NO_3^- increased steadily and reached a concentration of approximately 1016 μmol L^{-1} after 120 min. However, the total nitrogen of both NO_3^- and NO_2^- exceed that initially present in parathion. Air is another nitrogen source responsible for NO_3^- and NO_2^- ions formations in solution [52,53].

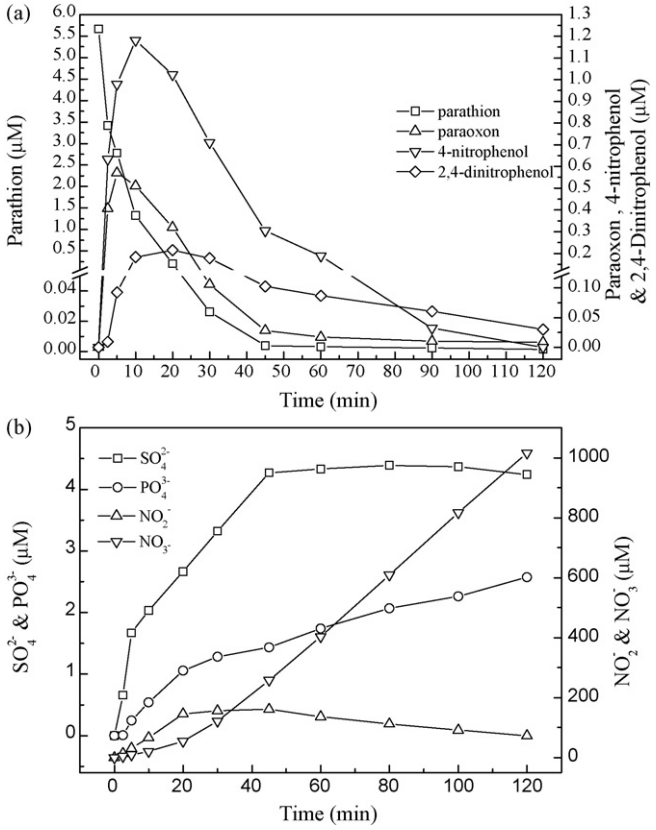

Fig. 4. Degradation of parathion and formation of main byproducts (ultrasonic power: 55.2 W; frequency: 600 kHz. (a) Organic byproducts; (b) inorganic byproducts.)

Table 2
GC–MS-EI retention time and spectral characteristics of parathion identified byproducts.

No.	Compounds name	CAS no.	Retention time (min)	Similarity (%)	Main characteristic ions (*m*/*z*)
1[a]	*p*-Benzoquinone	106-51-4	6.95	100	50, 54, 82, 108
2	Diethyl phosphite	762-04-9	7.733	95	45, 47, 65, 83, 93, 95, 109, 111
3[a]	Triethyl phosphate	78-40-0	11.117	100	81, 99, 109, 127, 155
4	O,O,O-triethyl thiophosphate	126-68-1	11.700	80	65, 81, 97, 109, 115, 121, 198
5	O,O,S-triethyl phosphorothioate	1186-09-0	13.975	86	45, 81, 109, 111, 138, 154, 170, 198
6	1-Ethoxy-4-nitro-benzene	100-29-8	17.050	80	65, 81, 93, 109, 139, 167
7[a]	2,4-Dinitrophenol	51-28-5	17.633	100	53, 63, 91, 107, 154, 184
8[a]	4-Nitrophenol	100-02-7	17.983	100	65, 81, 93, 109, 139
9	4-Nitrocatechol	3316-09-4	18.967	85	52, 81, 109, 125, 155
10[a]	Paraoxon	311-45-5	24.150	100	81, 109, 127, 139, 149, 247, 275
11[a]	Parathion	56-38-2	25.750	100	65, 97, 109, 125, 139, 155, 291

[a] Identified with standard samples.

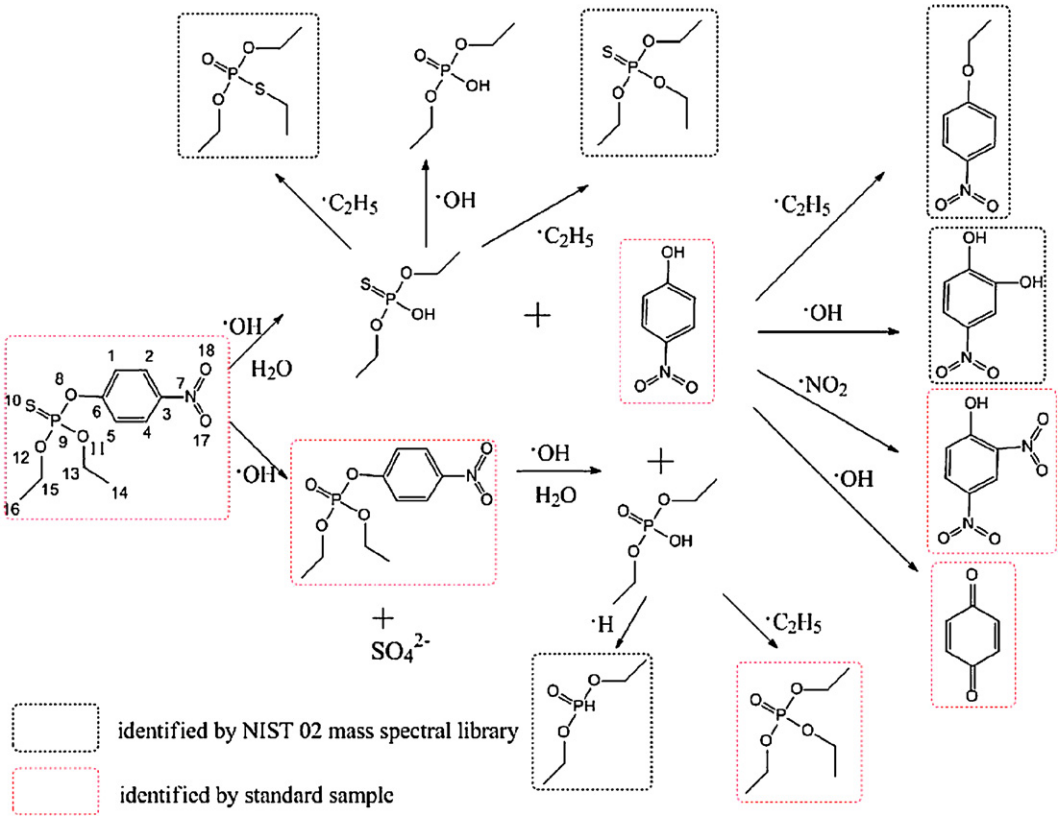

Fig. 5. Proposed main parathion degradation pathways under ultrasonic irradiation.

3.5. Mechanism of parathion degradation under ultrasonic irradiation

Based on the studies above, main parathion degradation pathways are proposed as shown in Fig. 5. The first step of parathion degradation under ultrasonic irradiation included: (1) the oxidative attack by •OH on the P=S bond, which results in the formation of paraoxon (compound 10) and SO_4^{2-}; (2) the oxidative attack by •OH on P–O bond which connects the thiophosphate group to the aromatic ring or the decomposition of *p*-nitrophenoxy caused by hydrolysis results in the formation of corresponding 4-nitrophenol (compound 8) and O, O-diethyl phosphorothioate.

The continuous attack of •OH on P–O bond of paraoxon and the hydrolysis of paraoxon results in the formation of the 4-nitrophenol (compound 8) and O, O-diethyl phosphonic ester.

O,O,O-triethyl thiophosphate (compound 4) and O,O,S-triethyl phosphorothioate (compound 5) could be formed through secondary ethylation of O, O-diethyl phosphorothioate. The sources of ethyl groups could come from decomposition of the small molecular organic acids or intermediates containing alcohol functional groups under ultrasonic irradiation. These byproducts were also reported in the photocatalytic and photolytic parathion degradations [50]. O,O,O-triethyl phosphate (compound 3) could come from the oxidation of O,O,O-triethyl thiophosphate (compound 4) or ethylation of O, O-diethyl phosphonic ester.

Due to the existent of abundant •H, O, O-diethyl phosphonic ester could be reduce to form diethyl phosphite (compound 2) [54].

The continuous attack of •OH on the benzene ring of 4-nitrophenol (compound 8) results in the formation of 4-nitrocatechol (compound 9) and 4-benzoquinone (compound 1), whereas the attack of $•NO_2$ could lead to the formation of 2,4-dinitrophenol. Its existent indicates that the N_2 in air may take part in the reaction through the conversion to $•NO_2$ under ultrasonic irradiation in presence of O_2 [52,53]. Therefore, the potential increase of inorganic even organic nitrogen caused by ultrasonic irradiation should be taken into account in the treatment process.

1-Ethoxy-4-nitro-benzene (compound 6) is formed by the attack of ethyl radical on OH group in 4-nitrophenol.

To support our conclusion that the sonochemical degradation of parathion is initiated with the thiophosphate-moiety oxidation, MO calculations were carried out by using Gaussian 03 program for the parathion molecule. Structures were optimized with the 6-31G(d) basis set at the level of the B3LYP, and then the frontier electron densities (FEDs) of the highest occupied molecular orbital (HOMO) and the lowest unoccupied molecular orbital (LUMO) were calculated. The evaluated FEDs are listed in Table 3.The atom serial number of parathion molecule is shown in Fig. 5.

Table 3
Frontier electron densities (FED) and point charge on heavy atoms of parathion.

No.	Atom	FED^2_{HOMO}	FED^2_{LUMO}	Point charge
1	C	0.001	0.004	0.024
2	C	0.004	0.076	0.029
3	C	0.001	0.057	0.284
4	C	0.003	0.075	0.027
5	C	0.004	0.004	0.016
6	C	0.001	0.099	0.366
7	N	0.000	0.260	0.376
8	O	0.050	0.012	−0.584
9	P	0.043	0.017	0.967
10	S	0.577	0.005	−0.395
11	O	0.012	0.000	−0.504
12	O	0.043	0.001	−0.495
13	C	0.003	0.000	0.304
14	C	0.000	0.000	0.036
15	C	0.002	0.000	0.301
16	C	0.000	0.000	0.036
17	O	0.000	0.189	−0.395
18	O	0.001	0.189	−0.394

On the basis of FED^2_{HOMO} values, the HOMO is located in thiophosphate moiety of parathion, while LUMO in the *p*-nitrophenoxy moiety. The position of O8, P9, O12, and S12 in thiophosphate moiety of parathion is electron-rich and most likely to be attacked by oxidants, especially for S10 with the value 10 times higher than the other three. Therefore, P=S bond is most readily attacked by •OH [55]. It is consistent with our conclusion the formation of paraoxon is the first and a main step of the parathion degradation. O8 and O12 are anther attacked positions of parathion by •OH. The attack of P-O8 band results in the formation of 4-nitrophenol, which is also in line with our conclusion the formation of 4-nitrophenol is the first but less main step. However, the byproducts formed by the attack of P-O12 were not detected in the GC–MS analysis.

The other pathway of parathion degradation is as a result of hydrolysis. The water molecules nucleophilically attack P atom which has the highest point charge to form a transition state and then the *p*-nitrophenoxy anion decomposed from parathion because the acidity of 4-nitrophenol is much strong than ethanol. This hydrolysis process can be enhanced under the ultrasonic irradiation.

4. Conclusion

1. At the conditions in question, degradation rate of parathion decreased with increasing initial concentration and decreasing power. The optimal frequency for parathion degradation was 600 kHz.
2. The free radical reactions predominate in the sonochemical degradation of parathion and the reaction zones are predominately at the interfacial regions between bubbles and bulk solution and, to a much lesser extent, in bulk solution.
3. The gas/liquid interfacial regions are the real effective reaction sites for sonochemical degradation of parathion. The reaction can be well described as a gas/liquid heterogeneous reaction which obeys a kinetic model based on Langmuir–Hinshelwood model.
4. The main pathways of parathion degradation by ultrasonic irradiation were also proposed. The N_2 in air takes part in the parathion reaction through the formation of $^{\bullet}NO_2$ under ultrasonic irradiation. Parathion is decomposed into paraoxon and 4-nitrophenol in the first step via two different pathways, respectively, which is in agreement with the theoretical molecular orbital calculation. However, the potential increase of inorganic even organic nitrogen caused by ultrasonic irradiation should be taken into account when ultrasonic applied in water treatment.

Acknowledgements

Support for the research has been provided by the National Major Project of Science & Technology Ministry of China (Grant No. 2008ZX07421-002) and National 11th Five-Year Plan Program (No. 2006BAJ08B06)

References

[1] Z. Zhang, H. Hong, X. Wang, J. Lin, W. Chen, L. Xu, Determination and load of organophosphorus and organochlorine pesticides at water from Jiulong River Estuary, China, Mar. Pollut. Bull. 45 (1–12) (2002) 397–402.
[2] M. Liess, R. Schulz, M.H.-D. Liess, B. Rother, R. Kreuzig, Determination of insecticide contamination in agricultural headwater streams, Water Res. 33 (1) (1999) 239–247.
[3] F. Tian, X. Wu, H. Pan, H. Jiang, Y. Kuo, A.M. Marini, Inhibition of protein kinase C protects against paraoxon-mediated neuronal cell death, Neurotoxicology 28 (4) (2007) 843–849.
[4] F. Monnet-Tschudi, M. Zurich, B. Schilter, L.G. Costa, P. Honegger, Maturation-dependent effects of chlorpyrifos and parathion and their oxygen analogs on acetylcholinesterase and neuronal and glial markers in aggregating brain cell cultures, Toxicol. Appl. Pharm. 165 (3) (2000) 175–183.
[5] K. Ohno, T. Minami, Y. Matsui, Y. Magara, Effects of chlorine on organophosphorus pesticides adsorbed on activated carbon: desorption and oxon formation, Water Res. 42 (6–7) (2008) 1753–1759.
[6] J. Wu, D.A. Laird, Abiotic transformation of chlorpyrifos to chlorpyrifos oxon in chlorinated water, Environ. Toxicol. Chem. 22 (2) (2003) 261–264.
[7] Y. Liu, D. Jin, X. Lu, P. Han, Study on degradation of dimethoate solution in ultrasonic airlift loop reactor, Ultrason. Sonochem. 15 (5) (2008) 755–760.
[8] M.A. Matouq, Z.A. Al-Anber, T. Tagawa, S. Aljbour, M. Al-Shannag, Degradation of dissolved diazinon pesticide in water using the high frequency of ultrasound wave, Ultrason. Sonochem. 15 (5) (2008) 869–874.
[9] R. Singla, F. Grieser, M. Ashokkumar, Sonochemical degradation of martius yellow dye in aqueous solution, Ultrason. Sonochem. 16 (1) (2009) 28–34.
[10] J. Lin, X. Zhao, D. Liu, Z. Yu, Y. Zhang, H. Xu, The decoloration and mineralization of azo dye C.I. Acid Red 14 by sonochemical process: rate improvement via Fenton's reactions, J. Hazard. Mater. 157 (2–3) (2008) 541–546.
[11] Y. Ohko, K. Iuchi, C. Niwa, T. Tatsuma, T. Nakashima, T. Iguchi, Y. Kubota, A. Fujishima, 17β-Estradiol degradation by TiO_2 photocatalysis as a means of reducing estrogenic activity, Environ. Sci. Technol. 36 (19) (2002) 4175–4181.
[12] M. Inoue, Y. Masuda, F. Okada, A. Sakurai, I. Takahashi, M. Sakakibara, Degradation of bisphenol A using sonochemical reactions, Water Res. 42 (6–7) (2008) 1379–1386.
[13] B. David, Sonochemical degradation of PAH in aqueous solution. Part I. Monocomponent PAH solution, Ultrason. Sonochem. 16 (2) (2009) 260–265.
[14] E. Psillakis, G. Goula, N. Kalogerakis, D. Mantzavinos, Degradation of polycyclic aromatic hydrocarbons in aqueous solutions by ultrasonic irradiation, J. Hazard. Mater. 108 (1–2) (2004) 95–102.
[15] J. Cheng, C.D. Vecitis, H. Park, B.T. Mader, M.R. Hoffmann, Sonochemical degradation of perfluorooctane sulfonate (PFOS) and perfluorooctanoate (PFOA) in landfill groundwater: environmental matrix effects, Environ. Sci. Technol. 42 (21) (2008) 8057–8063.
[16] C.D. Vecitis, H. Park, J. Cheng, B.T. Mader, M.R. Hoffmann, Kinetics and mechanism of the sonolytic conversion of the aqueous perfluorinated surfactants, perfluorooctanoate (PFOA), and perfluorooctane sulfonate (PFOS) into inorganic products, J. Phys. Chem. A 112 (18) (2008) 4261–4270.
[17] W. Song, K.E. O'Shea, Ultrasonically induced degradation of 2-methylisoborneol and geosmin, Water Res. 41 (12) (2007) 2672–2678.
[18] F. Méndez-Arriaga, R.A. Torres-Palma, C. Pétrier, S. Esplugas, J. Gimenez, C. Pulgarin, Ultrasonic treatment of water contaminated with ibuprofen, Water Res. 42 (16) (2008) 4243–4248.
[19] L. Sanchez-Prado, R. Barro, C. Garcia-Jares, M. Llompart, M. Lores, C. Petrakis, N. Kalogerakis, D. Mantzavinos, E. Psillakis, Sonochemical degradation of triclosan in water and wastewater, Ultrason. Sonochem. 15 (5) (2008) 689–694.
[20] W. Song, A.A. de La Cruz, K. Rein, K.E. O'Shea, Ultrasonically induced degradation of microcystin-LR and -RR: identification of products, effect of pH, formation and destruction of peroxides, Environ. Sci. Technol. 40 (12) (2006) 3941–3946.
[21] Y.G. Adewuyi, Sonochemistry: environmental science and engineering applications, Ind. Eng. Chem. Res. 40 (22) (2001) 4681–4715.
[22] Y.G. Adewuyi, Sonochemistry in environmental remediation. 1. Combinative and hybrid sonophotochemical oxidation processes for the treatment of pollutants in water, Environ. Sci. Technol. 39 (10) (2005) 3409–3420.
[23] M.R. Hoffmann, I. Hua, R. Höchemer, Application of ultrasonic irradiation for the degradation of chemical contaminants in water, Ultrason. Sonochem. 3 (3) (1996) S163–S172.
[24] M. Gutierrez, A. Henglein, F. Ibanez, Radical scavenging in the sonolysis of aqueous solutions of iodide, bromide, and azide, J. Phys. Chem. 95 (15) (1991) 6044–6047.
[25] A. Kotronarou, G. Mills, M.R. Hoffmann, Decomposition of parathion in aqueous solution by ultrasonic irradiation, Environ. Sci. Technol. 26 (7) (1992) 1460–1462.
[26] J. Wang, T. Ma, Z. Zhang, X. Zhang, Y. Jiang, D. Dong, P. Zhang, Y. Li, Investigation on the sonocatalytic degradation of parathion in the presence of nanometer rutile titanium dioxide (TiO_2) catalyst, J. Hazard. Mater. 137 (2) (2006) 972–980.
[27] J. Wang, Z. Pan, Z. Zhang, X. Zhang, F. Wen, T. Ma, Y. Jiang, L. Wang, L. Xu, P. Kang, Sonocatalytic degradation of methyl parathion in the presence of nanometer and ordinary anatase titanium dioxide catalysts and comparison of their sonocatalytic abilities, Ultrason. Sonochem. 13 (6) (2006) 493–500.
[28] J. Wang, W. Sun, Z. Zhang, X. Zhang, R. Li, T. Ma, P. Zhang, Y. Li, Sonocatalytic degradation of methyl parathion in the presence of micron-sized and nanosized rutile titanium dioxide catalysts and comparison of their sonocatalytic abilities, J. Mol. Catal. A: Chem. 272 (1–2) (2007) 84–90.
[29] T. Kimura, T. Sakamoto, J. Leveque, H. Sohmiya, M. Fujita, S. Ikeda, T. Ando, Standardization of ultrasonic power for sonochemical reaction, Ultrason. Sonochem. 3 (3) (1996) S157–S161.
[30] S. Koda, T. Kimura, T. Kondo, H. Mitome, A standard method to calibrate sonochemical efficiency of an individual reaction system, Ultrason. Sonochem. 10 (3) (2003) 149–156.
[31] M.A. Beckett, I. Hua, Impact of ultrasonic frequency on aqueous sonoluminescence and sonochemistry, J. Phys. Chem. A. 105 (15) (2001) 3796–3802.
[32] L. Yang, J.Z. Sostaric, J.F. Rathman, L.K. Weavers, Effect of ultrasound frequency on pulsed sonolytic degradation of octylbenzene sulfonic acid, J. Phys. Chem. B 112 (3) (2008) 852–858.
[33] C. Pétrier, A. Francony, Ultrasonic waste-water treatment: incidence of ultrasonic frequency on the rate of phenol and carbon tetrachloride degradation, Ultrason. Sonochem. 4 (4) (1997) 295–300.
[34] T. Lesko, A.J. Colussi, M.R. Hoffmann, Sonochemical decomposition of phenol: evidence for a synergistic effect of ozone and ultrasound for the

elimination of total organic carbon from water, Environ. Sci. Technol. 40 (21) (2006) 6818–6823.
[35] H. Hung, M.R. Hoffmann, Kinetics and mechanism of the sonolytic degradation of chlorinated hydrocarbons: frequency effects, J. Phys. Chem. A. 103 (15) (1999) 2734–2739.
[36] U.S. EPA, Health Effects Assessment for Parathion, EPA/600/8-88/047, Cincinnati, OH: Environmental Criteria and Assessment Office, Office of Health and Environmental Assessment, Office of Research and Development, 1988.
[37] K.E. O'Shea, A. Aguila, K. Vinodgopal, P.V. Kamat, Reaction pathways and kinetics parameters of sonolytically induced oxidation of dimethyl methylphosphonate in air saturated aqueous solutions, Res. Chem. Intermed. 24 (6) (1998) 695–705.
[38] K. Okitsu, K. Iwasaki, Y. Yobiko, H. Bandow, R. Nishimura, Y. Maeda, Sonochemical degradation of azo dyes in aqueous solution: a new heterogeneous kinetics model taking into account the local concentration of OH radicals and azo dyes, Ultrason. Sonochem. 12 (4) (2005) 255–262.
[39] K.I. Kim, O.J. Jung, Sonochemical decomposition of humic substances in wastewater effluent, Bull. Korean Chem. Soc. 22 (10) (2001) 1093–1100.
[40] N. Serpone, R. Terzian, H. Hidaka, E. Pelizzetti, Ultrasonic induced dehalogenation and oxidation of 2-, 3-, and 4-chlorophenol in air-equilibrated aqueous media. Similarities with irradiated semiconductor particulates, J. Phys. Chem. 98 (10) (1994) 2634–2640.
[41] C. Petrier, M. Lamy, A. Francony, A. Benahcene, B. David, V. Renaudin, N. Gondrexon, Sonochemical degradation of phenol in dilute aqueous solutions: comparison of the reaction rates at 20 and 487 kHz, J. Phys. Chem. 98 (41) (1994) 10514–10520.
[42] C.D. Vecitis, H. Park, J. Cheng, B.T. Mader, M.R. Hoffmann, Enhancement of perfluorooctanoate and perfluorooctanesulfonate activity at acoustic cavitation bubble interfaces, J. Phys. Chem. C 112 (43) (2008) 16850–16857.
[43] C. Liao, S. Kang, F. Wu, Hydroxyl radical scavenging role of chloride and bicarbonate ions in the H_2O_2/UV process, Chemosphere 44 (5) (2001) 1193–1200.
[44] B. Yim, Y. Nagata, Y. Maeda, Sonolytic degradation of phthalic acid esters in aqueous solutions. Acceleration of hydrolysis by sonochemical action, J. Phys. Chem. A 106 (1) (2002) 104–107.
[45] M. Sakakura, M. Takayama, Sonolytic hydrolysis of peptides in aqueous solution upon addition of catechol, Ultrason. Sonochem. 16 (3) (2009) 367–371.
[46] J.D. Schramm, I. Hua, Ultrasonic irradiation of dichlorvos: decomposition mechanism, Water Res. 35 (3) (2001) 665–674.
[47] Z. Frontistis, M. Papadakiand, D. Mantzavinos, Modelling of sonochemical processes in water treatment, Water Sci. Technol. 55 (12) (2007) 47–52.
[48] E. Evgenidou, I. Konstantinou, K. Fytianos, I. Poulios, T. Albanis, Photocatalytic oxidation of methyl parathion over TiO_2 and ZnO suspensions, Catal. Today 124 (3–4) (2007) 156–162.
[49] E. Moctezuma, E. Leyva, G. Palestino, H. de Lasa, Photocatalytic degradation of methyl parathion: reaction pathways and intermediate reaction products, Water Res. 186 (1) (2007) 71–84.
[50] C. Wu, K.G. Linden, Degradation and byproduct formation of parathion in aqueous solutions by UV and UV/H_2O_2 treatment, Water Res. 42 (19) (2008) 4780–4790.
[51] T. Kim, J. Kim, K. Choi, M.K. Stenstrom, K. Zoh, Degradation mechanism and the toxicity assessment in TiO_2 photocatalysis and photolysis of parathion, Chemosphere 62 (6) (2006) 926–933.
[52] V. Mišík, P. Riesz, Nitric oxide formation by ultrasound in aqueous solutions, J. Phys. Chem. 100 (45) (1996) 17986–17994.
[53] G. Mark, H. Schuchmann, C. von Sonntag, Formation of peroxynitrite by sonication of aerated water, J. Am. Chem. Soc. 122 (15) (2000) 3781–3782.
[54] R. Wu, C. Chen, M. Chen, C. Lu, Titanium dioxide-mediated heterogeneous photocatalytic degradation of terbufos: parameter study and reaction pathways, J. Hazard. Mater. 162 (2–3) (2009) 945–953.
[55] N. Watanabe, S. Horikoshi, H. Kawabe, Y. Sugie, J. Zhao, H. Hidaka, Photodegradation mechanism for bisphenol A at the TiO_2/H_2O interfaces, Chemosphere 52 (5) (2003) 851–859.